

The role of $4f$ electrons in the stopping power of hafnium

C. C. Montanari,* A. M. P. Mendez, D. M. Mitnik, and J. E. Miraglia
*Instituto de Astronomía y Física del Espacio, Consejo Nacional de Investigaciones Científicas
y Técnicas - Universidad de Buenos Aires, Pabellón IAFE, 1428 Buenos Aires, Argentina*

P.A. Miranda, R. Correa, J. Wachter, and M. Aguilera
*Departamento de Física, Facultad de Ciencias Naturales,
Matemática y del Medio Ambiente. Universidad Tecnológica Metropolitana. 7800002, Chile*

E. Alves
*Centro de Ciências e Tecnologias Nucleares, Instituto Superior Técnico,
Universidade de Lisboa, 2696-953 Sacavém, Portugal and
Instituto de Plasma e Fusão Nuclear, Instituto Superior Técnico,
Universidade de Lisboa, 2696-953 Sacavém, Portugal*

N. Catarino and R.C. da Silva
*Centro de Ciências e Tecnologias Nucleares, Instituto Superior Técnico,
Universidade de Lisboa, 2696-953 Sacavém, Portugal*
(Dated: February 20, 2020)

The stopping power of protons through Hf foil has been studied both experimentally and theoretically. The measurements were performed at the Laboratory of Accelerators and X-Ray Diffraction in Lisbon, by using the transmission method on self-supporting stopping material, for (0.6-2.5) MeV protons. The theoretical developments involved fully relativistic atomic structure calculations for Hf, which required the solution of the Dirac equation. The shell-wise local plasma approximation (SLPA) was used to describe the energy transferred to the bound $1s$ - $4f$ electrons, and the outer four electrons were considered as a free electron gas (FEG). We found the relativistic description of the $4f$ -shell, and the screening between $4f$ and $5p$ electrons, are decisive around the stopping maximum. The present theoretical and experimental results have very good agreement in the energy region of the new measurements. However, our theoretical stopping cross sections show substantial differences with the semi-empirical models, such as SRIM2013 and ICRU-49, at intermediate to low energies. Our calculations suggest the stopping maximum to be larger, and shifted to lower energies, respect to these semi-empirical models. Future measurements below 100 keV would be required to validate our predictions.

I. INTRODUCTION

For impact energies above a few keV/amu, mono-energetic charged particles penetrating a foil of any material lose their energy through a series of consecutive inelastic collisions, mainly with target electrons^{1,2}. The information given by the energy loss process is essential not only to have a better knowledge of the phenomena behind the fundamental interactions but also because it plays an important role in many applied fields such as materials science, nuclear physics, ionic implantation, and radiotherapy^{2,3}. Experimental data in ion mean energy loss per unit path $S(E)$ is of crucial relevance to check the reliability of semi-empirical models and to determine some key parameters⁴⁻⁶. However, often, the experimental data available is rather scarce, which is troublesome when the material under study corresponds to an element of low occurrence on the Earth's upper crust, such as Hf.

So far, only one experimental work has been published regarding the stopping power cross section of pure hafnium for protons⁷, while more attention has been recently given to studies involving hafnium oxide because of its practical use⁸⁻¹⁰. It is well known that significant attention has been paid in recent years to transi-

tion metal-oxides such as HfO_2 because of their potential as alternative gate dielectrics to replace SiO_2 for the future generation of nano-electronics with less than 45 nm gate length^{11,12}. Some important physical properties of the above mentioned metal-oxide films depend on its thickness, which is often measured by using Rutherford Backscattering Spectrometry^{13,14}, a method that relies heavily on the determination of the stopping power of ion beams in the material of interest.

In this study, we report experimental stopping power cross section values over the incident energy range (0.6-2.5) MeV for protons crossing self-supported Hf thin-film by using the transmission method. We aim not only to upgrade stopping power data compilations^{15,16} but also to provide useful information about the processes governing the slowing down of protons in multi-electronic targets. In the rare earth metals, the $4f$ electrons play a relevant role in the stopping power, being the first shell of bound electrons below the conduction band. As already noted¹⁷, the free electron gas (FEG) shows unexpected behavior in these elements, which casts doubts on its proper description. With Hf, we found the contribution of the $4f$ -shell decisive even at impact energies around the stopping maximum, as shown later.

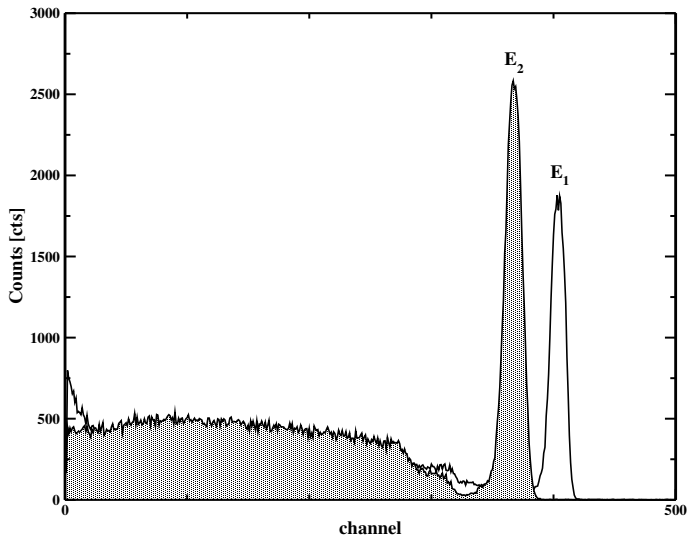


FIG. 1. RBS spectrum for $E_{avg} = 921.1$ keV protons on hafnium sample, which is subsequently used to determine the energy loss in the foil.

The theoretical approach implemented in this work uses the shell-wise local plasma approximation (SLPA)²⁰, to describe the energy transferred to the bounds 1s-4f electrons, and two different models for the FEG: the screened potential with cusp condition model (SPCC)²¹, which is non-linear binary formalism; and the Mermin-Lindhard dielectric formalism (ML)²², for energies around the stopping maximum and above. Our model requires the relativistic description of the wave functions and binding energies of Hf¹⁸, where we consider 4 electrons per atom in the FEG. The 14 electrons occupying the 4f subshell of Hf makes up the main contribution to the stopping below the FEG, which causes the cross sections to be very sensitive to a good description of this shell. The screening between the 4f and 5p electrons has been considered, and it has been found to play a major role within the SLPA predictions.

The experimental details and data are given in Section II, while the theoretical method is explained in Section III. Present theoretical and experimental values are finally compared to the available experimental values⁷, the ICRU-49 calculations²³, and the SRIM-2013 package²⁴. Conclusions and discussions are given in section V.

II. EXPERIMENTAL ARRANGEMENTS

A. Accelerator and scattering Chamber

The procedure used in this work to obtain stopping power data is essentially the same as described in reference²⁵. However, this time the measurements were made at the IST/LATR (Laboratory of Accelerators and X-Ray Diffraction) in Lisbon. This facility uses a 2.5 MV Van de Graaff accelerator to deliver $^1\text{H}^+$ primary

ion beams through a series of electrostatic lenses and collimators onto a thin Au/SiO₂ sample which is used as a scattering center. This sample was placed in the center of a RBS/C scattering chamber where a high vacuum (pressure of $\sim 10^{-6}$ Torr) was maintained during the measurements. The beam current on sample was kept at around 5.0 nA in order to attain sufficient statistics in each particle spectrum. By using a beam spot of about 1.0 mm in diameter, a solid angle of 11.4 msr was attained. The overall energy resolution (FWHM) of the detection system was about 15 keV relative to 5.486 MeV alpha particles from a ^{241}Am source.

B. Target

The stopping material under analysis was a hafnium foil with nominal thickness of $1.0 \mu\text{m}$ and 99.95% purity which was supplied by Lebow Company²⁶. However, a more precise thickness value was achieved by measuring the energy loss of alpha particles coming from a calibrated (^{239}Pu , ^{241}Am , ^{244}Cm) source. From the alpha spectra with and without the Hf foil interposed, the characteristic energy shift δE was measured and then combined with the stopping power for 5.486 MeV alphas on hafnium ($55.69 \text{ eV}/10^{15} \text{ at}/\text{cm}^2$) found in Ref.²⁴ in order to obtain an areal density of $(4.13 \pm 0.21) \times 10^{19} \text{ at}/\text{cm}^2$ which corresponds to a thickness of $0.920 \pm 0.046 \mu\text{m}$.

C. Energy loss measurement

Once the beam impinges on the Au/SiO₂ sample, protons are backscattered towards a Si surface barrier detector located at 140° relative to the initial beam direction. Fig.1 shows two particle spectra where ion energies E_2 and E_1 are associated to a placed and removed hafnium sample, respectively. Both energy distributions were fitted by gaussian functions to obtain the mean energy and width (FWHM) of the peaks²⁷, and from the difference between these two peak positions in the spectrum, the total energy loss $\Delta E = (E_1 - E_2)$ in the foil was calculated. As established in previous studies^{5,25}, the experimental stopping powers cross sections $\varepsilon(E)$ are determined at some mean energy E_{avg} by measuring the ion energy losses ΔE within the investigated Hf foil which has a mean thickness denoted by Δx . In this way, only when the energy loss fraction $\Delta E/E_{avg}$ across the Hf foil is not exceeding 20% it is possible to define the stopping cross section by^{28,29}:

$$\varepsilon(E) = \frac{S(E)}{N} = -\frac{dE}{N dx} \approx -\frac{\Delta E}{N \Delta x}, \quad (1)$$

where N denotes the atomic number density (atoms cm^{-3}) of the material under study. When this condition was not fulfilled, a small correction to the mean energies E_{avg} was applied in order to account for the nonlinear dependence on ion energy of stopping powers^{30,31}.

III. THEORETICAL METHOD

The energy loss of ions in metal targets responds to different physical mechanisms, depending on the impact ion velocity. At low velocities the binary collisions are responsible of the loss of energy by the ion. The main contribution is the ionization of electrons of the metal conduction band, which is well approximated by a free electron gas (FEG) of Fermi velocity v_F . Instead, above certain velocity (i.e. $v \geq 1.5 v_F$), not only binary but also collective excitations (plasmons) are possible²¹. At high energies, not only the FEG contributes to the stopping power but also the bound electrons. The method used in this work combines a description for the interaction with the valence (or conduction) electrons as a FEG, and a different one for the interaction with the bound electrons.

We used the SPCC model²¹ to describe the stopping power of low velocity charged particles in the FEG. It is a non-perturbative binary collisional model, thus valid at energies below that of plasmon excitations. The SPCC²¹ is based on a screened central potential with cusp condition of the electronic density close to the projectile. It proved to give a good description of the induced electron density even for negative projectiles²¹, and reproduces the low velocity proton-antiproton differences in the stopping power (Barkas effect). The SPCC formalism only depends on the Wigner-Seitz radius, r_S , which is a measure of the electronic density of the FEG. For metals of well-known value of r_S , the SPCC describes very well the low energy experimental stopping data²¹, agreeing with the DFT results by Echenique and coworkers^{32,33} at $v = 0$.

Hafnium ($Z=72$, [Xe] $4f^{14} 6s^2 5d^2$), belongs to the first groups of transition metals, with 4 electrons as FEG (theoretical $r_S = 2.14$ a.u.) and $1s-4f$ electrons bound. We checked the r_S value with the experimental one obtained from measured energy loss function by Lynch *et al*³⁴. The experimental plasmon energy of Hf is $\hbar\omega_P \approx 15.8$ eV, with a width at half maximum $\delta \approx 4.4$ eV, and $r_S \approx 2.07$ a.u.³⁴. Following²¹, the difference of less than 5% between theoretical and experimental r_S assess Hf as a canonical target.

Above certain impact velocity the plasmon contribution is important (i.e. around and above the stopping maximum). An interesting value for our analysis is the minimum impact velocity to excite plasmons, v_P . In the dielectric formalism this value can be obtained as $v_P \approx v_F[1 + (3\pi v_F)^{-1/2}]^{35}$. To describe the energy loss considering collective and binary excitation we resort to the ML dielectric formalism²², which is a linear response, perturbative approximation, so it depends on the square of the ion charge. In this formalism, the response of target electrons to the ion passage is described through the quantum dielectric function, depending on the characteristic r_S and δ parameters of the FEG.

For the stopping power due to bound electrons, the SLPA^{20,21} is employed. It is worth to mention that the

only inputs for the SLPA are the space-dependent densities of each shell in the ground state, and their binding energies. Collective processes and screening among electrons are included. Hafnium is a relativistic target, therefore the wave functions and binding energies must be obtained as solutions of Dirac equation¹⁸.

Figure 2 (a) shows non relativistic and our relativistic binding energies $E_{nl\pm}$, where $\pm = j \pm 1/2$. We compare our results with experimental measurements on solid Hf¹⁹ from $1s$ to $4f_{\pm}$. We notice that not only the deep shells require relativistic calculations, but also the outer $5p$ and $4f$ shells. Figure 2 (b) displays the relative error of non relativistic and relativistic energies with respect to the experimental data in logarithmic scale. This figure shows very clearly the disability of non-relativistic calculations to describe the experimental data, which surprisingly worsens from the inner to the outer shells.

Our relativistic binding energies present spin-orbit split. However, in total stopping power where the initial state of the excited electron is not measured, the quantum uncertainty in energy ΔE melts this split. The criteria $\Delta E \Delta t \geq \hbar/2$ merges the energies $E_{nl+} - E_{nl-}$ for sufficiently small values of Δt (the collisional mean-time). In fact, at sufficiently high impact velocity we can expect all target electrons to respond together to the ion passage^{36,37}. As in³⁸, the collisional time was estimated as follows $\Delta t \approx \langle r_i \rangle / v$, with $\langle r_i \rangle$ and v being the orbital mean radius and impact velocity, respectively.

The SLPA calculates the contribution of each subshell of bound electrons to the total stopping cross sections. We found that for every sub-shell of Hf, at the impact energy at which this sub-shell began to contribute, the spin-orbit split was unresolved. Then the nl -electrons should be considered together, responding to the ion passage as a single gas of electrons with density $\delta_{nl}(r)$ and a mean binding energy E_{nl} . This is important within the SLPA calculations because of the screening among electrons of the *same* binding energy. For example, the $4f_-$ and $4f_+$ of Hf can only be resolved for impact energies $E < 0.05$ keV, but the contribution of $4f$ to the total stopping is negligible if $E < 40$ keV. Moreover, the $5p$ and $4f$ electrons of Hf are very close in energy ($\Delta E_{5p-4f} \approx 1$ a.u.¹⁸) and react together for impact energies $E > 40$ keV (inter-shell screening).

In figure 3 we display the present theoretical stopping cross section of Hf for protons with and without the $5p-4f$ screening. We added the FEG and the bound electron contributions as explained above. The minimum energy for plasmon excitation was estimated as 37 keV. We used the non-perturbative SPCC model for impact energies $E \leq 37$ keV, and the perturbative ML calculation above this energy. Clearly, considering $5p-4f$ electrons as a single group of 20 electrons with screening among them gives lower stopping values than the addition of the separate $5p$ and $4f$ contributions. This is a shell correction that can only be considered within a many electron model such as the SLPA.

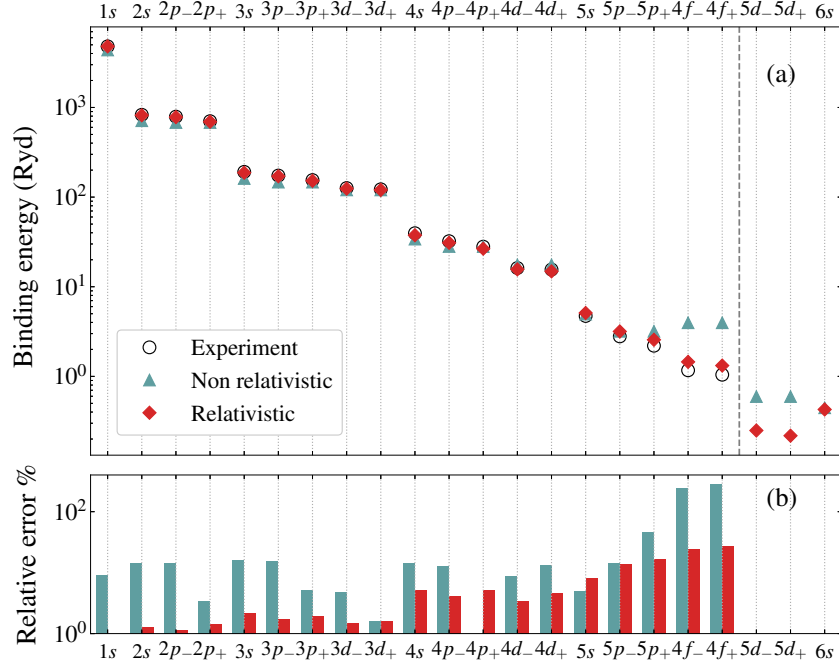


FIG. 2. (a) Binding energies of Hf. Non relativistic and relativistic calculations are given with filled symbols. Experimental measurements for solids¹⁹ are depicted with hollow circles. (b) Corresponding relative errors respect to experimental data.

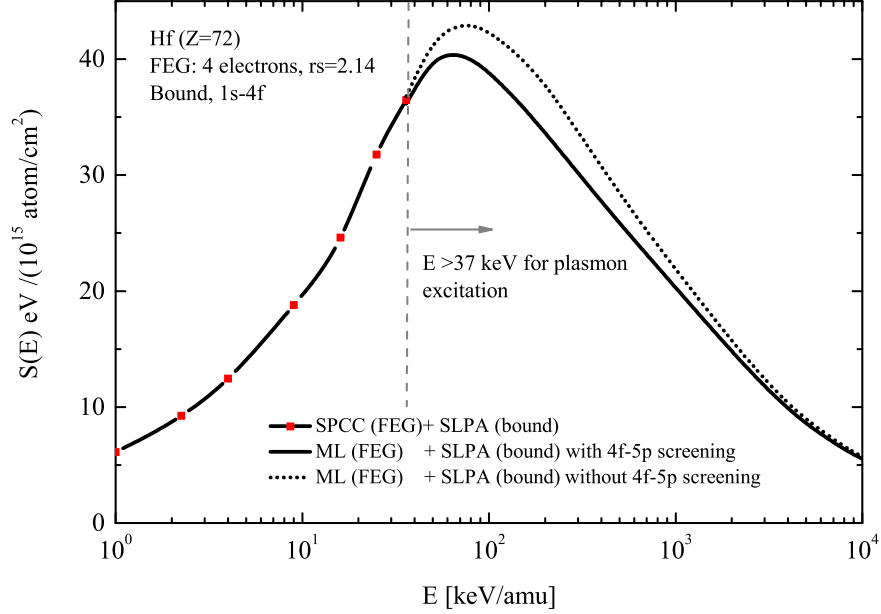


FIG. 3. Theoretical total stopping cross sections of protons in hafnium adding FEG and bound 1s-4f contributions, as mentioned in the inset. The vertical grey dashed-line indicates the energy above which plasmon excitation is possible. The SLPA calculations for 1s-4f bound electrons with and without 5p – 4f screening give different total stopping values, displayed with solid and dotted lines, respectively.

IV. ANALYSIS OF THE RESULTS AND DISCUSSION

The present data and theoretical results are displayed in table I, and figure 4. As can be seen in Table I, an

overall relative uncertainty of around 5% was achieved for the experimental stopping power values, mainly due to the uncertainty in the hafnium foil thickness.

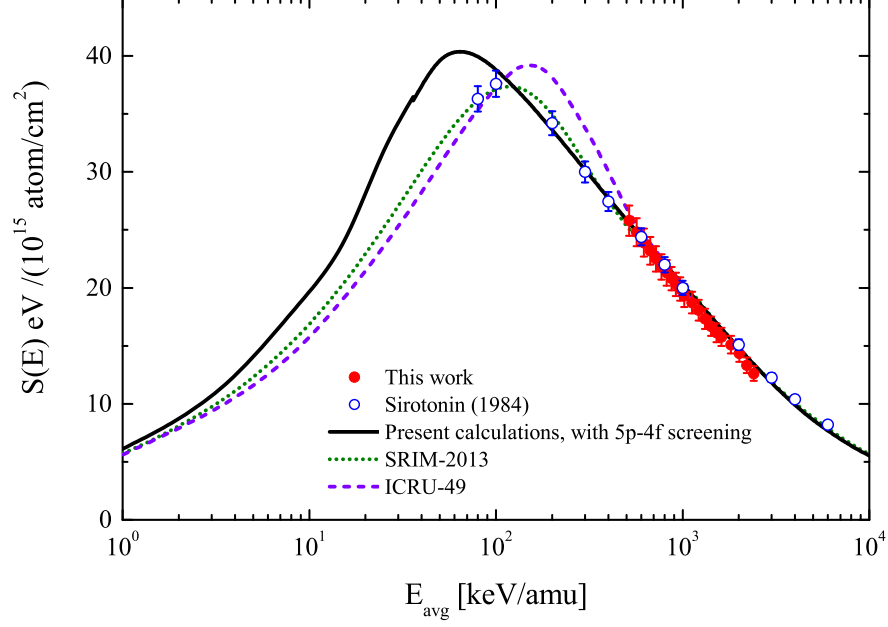


FIG. 4. Stopping power cross section of hafnium for protons. Symbols: solid circles, present values; open circles, previous data⁷. Curves: Black solid-line, present full theoretical results with $4f$ - $5p$ screening; violet dashed-line, values from ICRU-49²³, and green dotted line, SRIM-2013²⁴.

TABLE I. Stopping power values S_{exp} of hafnium for protons measured in this work. $\Delta E/E$ values are also shown.

E_{avg} keV	S_{exp} eV/(10^{15} at/cm ²)	$\Delta E/E$ %	E_{avg} keV	S_{exp} eV/(10^{15} at/cm ²)	$\Delta E/E$ %	E_{avg} keV	S_{exp} eV/(10^{15} at/cm ²)	$\Delta E/E$ %
516,6	$25,8 \pm 1,3$	20,5	1170,3	$18,25 \pm 0,91$	6,4	1813,4	$15,10 \pm 0,76$	3,4
567,8	$24,8 \pm 1,2$	17,9	1220,0	$18,08 \pm 0,90$	6,1	1862,7	$14,79 \pm 0,74$	3,3
618,8	$23,9 \pm 1,2$	15,8	1269,6	$17,57 \pm 0,88$	5,7	1912,0	$14,21 \pm 0,71$	3,0
669,6	$23,2 \pm 1,2$	14,2	1319,2	$17,32 \pm 0,87$	5,4	1961,2	$14,46 \pm 0,72$	3,0
720,1	$22,5 \pm 1,1$	12,8	1368,8	$17,15 \pm 0,86$	5,1	2010,4	$14,34 \pm 0,72$	2,9
770,5	$21,8 \pm 1,1$	11,6	1418,3	$16,69 \pm 0,83$	4,8	2059,6	$13,76 \pm 0,69$	2,7
820,8	$21,3 \pm 1,1$	10,7	1467,8	$16,43 \pm 0,82$	4,6	2108,8	$13,78 \pm 0,69$	2,7
871,0	$20,8 \pm 1,0$	9,8	1517,2	$16,13 \pm 0,81$	4,4	2158,0	$13,70 \pm 0,69$	2,6
921,1	$20,3 \pm 1,0$	9,1	1566,7	$16,04 \pm 0,80$	4,2	2206,5	$13,33 \pm 0,67$	2,5
971,1	$19,9 \pm 1,0$	8,4	1616,0	$15,77 \pm 0,79$	4,0	2256,4	$13,27 \pm 0,66$	2,4
1021,0	$19,33 \pm 0,97$	7,8	1665,4	$15,51 \pm 0,78$	3,8	2305,5	$13,07 \pm 0,65$	2,3
1070,8	$19,03 \pm 0,95$	7,3	1714,8	$15,46 \pm 0,77$	3,7	2354,7	$12,91 \pm 0,65$	2,2
1120,6	$18,73 \pm 0,94$	6,9	1764,1	$14,93 \pm 0,75$	3,5	2403,8	$12,61 \pm 0,63$	2,2

There is good agreement between the present theoretical results, the new data in Table I, and also with previous data by Sirotonin⁷, except for the lowest energy measurement at 80 keV. It is interesting that our full theoretical curve differs from SRIM-2013 one for impact energies below 100 keV. We obtain a stopping maximum around $40 \cdot 10^{-15}$ eV cm²/atom at 65 keV. Instead, following the up-to-now only set of data⁷, SRIM-2013 sug-

gests a lower stopping maximum at impact energy of 115 keV. It is worth to mention that similar theoretical results using the experimental $r_S = 2.07$ a.u. instead of the theoretical $r_S = 2.14$ a.u. give the stopping maximum at the same impact energy but 4% higher. Future experiments for impact energies below 100 keV would be important to complete this study.

V. CONCLUSION

In this work, we have used the transmission method to experimentally determine stopping power cross section values for (0.6-2.5) MeV protons incident on self-supporting Hf foils with an overall uncertainty of around 5%. Additionally, we calculated values extracted from the theoretical framework that involved the relativistic wave functions and binding energies of Hf, and considered 4 electrons per atom in the free electron gas. The shell-wise local plasma approximation was employed to describe the energy transferred to the bound 1s-4f electrons, and two different models for the FEG: the screened potential with cusp condition (SPCC model) for energies below that of the plasmon excitation, and the Mermin-Lindhard dielectric formalism, for energies around the stopping maximum and above. Present theoretical stopping cross sections cover an extensive energy range from 1 keV/amu-10 meV/amu.

At high impact energies, the new stopping measurements are in good agreement with our theoretical re-

sults, and also with already published experimental data and semi-empirical values calculated by means of SRIM-2013 and ICRU-49. However, we call the attention that around the stopping maximum and at lower impact energies the difference between our full-theoretical results and SRIM is substantial. To our knowledge, these are the first theoretical calculations of stopping in Hf taking into account the atomic relativistic effect. Future experiments for impact energies below 100 keV would be important to complete this study.

ACKNOWLEDGMENTS

This work was funded by VRAC Grant Number L1-17 of Universidad Tecnológica Metropolitana, Chile; also by the Consejo Nacional de Investigaciones Científicas y Técnicas (CONICET), the Agencia Nacional de Promoción Científica y Tecnológica (ANPCyT), and Universidad de Buenos Aires (UBA), of Argentina.

The authors gratefully acknowledge the invaluable contribution of F. Baptista from ITN/IST-UTL, Sacavém, Portugal for his constant availability.

-
- * mclaudia@iafe.uba.ar
- ¹ W.K. Chu, J.W. Mayer, M.A. Nicolet (Eds.) Backscattering Spectrometry, Academic Press, New York, 1978.
 - ² P. Sigmund, "Particle Penetration and Radiation Effects. General Aspects and Stopping of Swift Point Charges". Springer Series in Solid-State Sciences, Vol. 151, Springer, Berlin (2006).
 - ³ D. Schardt, T. Elsässer, D. Schulz-Ertner, Rev. Mod. Phys. **82**, 383-425 (2010).
 - ⁴ P.K. Diwan, S. Kumar, Nucl. Instr. and Meth. B **359**, 78-84 (2015).
 - ⁵ D. Moussa, S. Damache and S. Ouichaoui, Nucl. Instr. and Meth. B **268**, 1754-1758 (2010); **343**, 44-47 (2015).
 - ⁶ S. Damache, S. Ouichaoui, A. Belhout, A. Medouni and I. Toumert, Nucl. Instr. and Meth. B **225**, 449-463 (2004).
 - ⁷ E.I. Sirotnin, A.F. Tulinov, V.A. Khodyrev, V.N. Mizgulin, Nucl. Instr. and Meth. B **4**, 337-345 (1984).
 - ⁸ I. Abril, M. Behar, R. García Molina, R.C. Fadanelli, L.C.C.M. Nagamine, P.L. Grande, L. Schünemann, C.D. Denton, N.R. Arista, E.B. Saitovich, Eur. Phys. J. D **54**, 65-70 (2009).
 - ⁹ M. Behar, R.C. Fadanelli, I. Abril, R. García-Molina, C.D. Denton, L.C.C.M. Nagamine, N.R. Arista, Phys. Rev. A **80**, 062901 (2009).
 - ¹⁰ D. Primetzhofer, Nucl. Instr. and Meth. B **320**, 100-103 (2014).
 - ¹¹ J.H. Choi, Y. Mao, J.P. Chang, Mat. Sci. Eng. R **72**, 97-136 (2011).
 - ¹² J. Robertson, R.M. Wallace, Mat. Sci. Eng. R **88**, 1-41 (2015).
 - ¹³ Z.B. Alfassi, "Non-destructive elemental analysis", Blackwell Science Ltd. (2001).
 - ¹⁴ J.R. Tesmer, M. Nastasi, J.C. Barbour, C.J. Maggiore and J.W. Mayer, "Handbook of Modern Ion Beam Material Analysis", Materials Research Society (1995).
 - ¹⁵ <https://www.nds.iaea.org/stopping/>.
 - ¹⁶ C.C. Montanari, and P. Dimitriou, Nucl. Instr. and Meth. B **408**, 50-55 (2017).
 - ¹⁷ D. Roth, B. Bruckner, M. V. Moro, S. Gruber, D. Goebel, J. I. Juaristi, M. Alducin, R. Steinberger, J. Duchoslav, D. Primetzhofer, and P. Bauer, Phys. Rev. Lett **118**, 103401 (2017).
 - ¹⁸ A.M.P. Mendez, C.C. Montanari, D.M. Mitnik, Nucl. Instrum. Meth. B **460**, 114-118 (2019).
 - ¹⁹ G. Williams in <http://xdb.lbl.gov/Section1/Sec.1-1.html>
 - ²⁰ C.C. Montanari and J.E. Miraglia, Adv. Quant. Chem. **65**, edited by Dz. Belkic (Elsevier, Amsterdam, 2013), Chap. 7, pp. 165-201.
 - ²¹ C.C. Montanari, and J.E. Miraglia, Phys. Rev. A **96**, 012707 (2017).
 - ²² N.D. Mermin, Phys. Rev. B **1**, 2362 (1970).
 - ²³ ICRU report 49, Stopping Powers and Ranges for Protons and Alpha Particles, International Commission on Radiation Units and Measurements, 1993.
 - ²⁴ J.F. Ziegler, J.P. Biersack, SRIM2013, Computer Program and Manual. Available from www.srim.org.
 - ²⁵ P.A. Miranda, A. Sepúlveda, J.R. Morales, T. Rodríguez, E. Burgos, H. Fernández, Nucl. Instr. and Meth. B **318**, 292-296 (2014).
 - ²⁶ Lebow Company. 5960 Mandarin Ave. Goleta CA, 93117, USA.
 - ²⁷ G. Sun, M. Döbelli, A.M. Müller, M. Stocker, M. Suter and L. Wacker, Nucl. Instr. and Meth. B **256**, 586-590 (2007).
 - ²⁸ J. Raisanen, U. Watjen, A.J.M. Plompen, F. Munnik, Nucl. Instr. and Meth. B **118** (1996) 1-6.
 - ²⁹ F. Schulz and J. Shchuchinzky, Nucl. Instr. and Meth. B **12**, 90-94 (1985).
 - ³⁰ A.B. Chilton, J.N. Cooper and J.C. Harris, Phys. Rev. **93**,

- 413-418 (1954).
- ³¹ M. Rajatora, K. Vakevainen, T. Ahlgre, E. Rauhala, J. Raisanen, K. Rakennus, Nucl. Instr. and Meth. B **119**, 457-462 (1996).
 - ³² P. M. Echenique, R. M. Nieminen and R. H. Ritchie, Sol. State Comm. **37**, 779-781 (1981).
 - ³³ I. Nagy, A. Arnau, P. M. Echenique, and E. Zaremba, Phys. Rev. B **40**, 11986 (1989).
 - ³⁴ D. W. Lynch, C. G. Olson, and J. H. Weaver, Phys. Rev. B **11**, 3617-3624 (1975).
 - ³⁵ C. C. Montanari, J. E. Miraglia, and N. R. Arista, Phys. Rev. A **62**, 052902 (2000).
 - ³⁶ J. Lindhard, M. Scharff, Mat. Fys. Medd. Dan. Vid. Selsk **27**, 1 (1953).
 - ³⁷ W. K. Chu, D. Powers, Rev. Lett. A **40**, 23 (1972).
 - ³⁸ C.C. Montanari, D.M. Mitnik, C.D. Archubi, and J.E. Miraglia, Phys. Rev. A **80**, 012901 (2009).